Fluorescent Micelles Based on Star Amphiphilic Copolymer with a Porphyrin Core for Bioimaging and Drug Delivery[a]

Luzhong Zhang, Ying Lin, Yajun Zhang, Rui Chen, Zhenshu Zhu, Wei Wu,* Xiqun Jiang*

Star-shaped poly(ε-caprolactone)-*b*-poly(ethylene oxide) amphiphilic copolymer with a tetrakis-(4-aminophenyl)-terminated porphyrin core was synthesized. Paclitaxel (PTX)-loaded polymeric micelles were prepared by the self-assembly of the star copolymer and in situ encapsulation of PTX. The fluorescent characteristic of the porphyrin moiety allowed the cellular uptake and biodistribution of the PTX-loaded micelles to be monitored by fluorescent imaging. The PTX-loaded micelles can be readily internalized by cancer cells and have a slightly higher cytotoxicity than clinic PTX injection Taxol. In vivo real-time fluorescent imaging revealed that the micelles could accumulate at tumor site via the blood circulation in tumor-bearing mice. In vivo antitumor efficacy examinations indicated that the PTX-loaded micelles had significantly superior efficacy in impeding tumor growth than Taxol and low toxicity to the living mice.

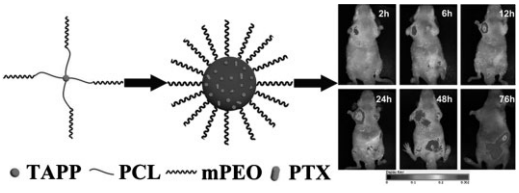

Introduction

The biodegradable and biocompatible amphiphilic copolymers have been attracting great attentions in the applications of drug delivery.[1,2] The amphiphilic copolymers can self-assemble into micelles consisting of hydrophobic core and hydrophilic shell in aqueous solution.[3] The polymeric micelles have significant advantages in drug delivery, such as improving the solubility of hydrophobic drugs, controlling the drug release rate, enhancing the therapeutic effects and weakening the side effects of drugs.[4] However, the polymeric micelles are frequently dissociated after systemic injection due to the blood flow dilution and fluid shear stress, when the micelles are not effectively cross-linked.[5] Consequently, the drug trapped in the micelles will be released prematurely before reaching the lesion site. Therefore, the physical stability of the drug-loaded polymeric micelles becomes one of the most crucial factors influencing their therapeutic activity.[6]

The polymeric micelles prepared by star-shaped copolymers have been demonstrated to be more thermodynamically stable than the micelles prepared by linear copolymer,[7–11] since the critical aggregation concentration value of star shaped copolymer is lower than that of linear counterparts.[12] This characteristic makes the star shaped copolymer promising in the formulation of polymeric micelles for drug and gene delivery.[13–19] Since the porphyrin moiety is biocompatible, porphyrin derivatives with multiple functional groups at their periphery are desirable cores for synthesizing star shaped amphiphilic copolymers. For example, poly(ε-caprolactone)-*b*-poly(oligo(ethylene glycol) methyl ether methacrylate) copolymer

L. Zhang, Y. Lin, Y. Zhang, R. Chen, Z. Zhu, W. Wu, X. Jiang
Laboratory of Mesoscopic Chemistry and Department of Polymer Science & Engineering, College of Chemistry & Chemical Engineering, Nanjing University, Nanjing 210093, P. R. China and Jiangsu Provincial Laboratory for Nanotechnology, Nanjing University, Nanjing 210093, P. R. China
E-mail: jiangx@nju.edu.cn, wuwei@nju.edu.cn

[a] **Supporting Information** for this article is available at Wiley Online Library or from the author.

DOI: 10.1002/mabi.201100197

with porphyrin as a core was synthesized.[20] Additionally, porphyrin can bring about new functions, such as energy transfer, intense fluorescence, photothermal therapy and fluorescent imaging.[21–25] By taking advantage of the photoacoustic and fluorescent properties of porphyrin, the vesicles prepared from the amiphiphilic molecule containing porphyrin have been used in the imaging of lymphatic systems and tumor.[26] Also, the photothermal characteristic of porphyrin in the vesicles under the laser irradiation has been used for tumor treatment.[26]

In the present work, we report the PTX-loaded fluorescent micelles based on star-shaped poly(ε-caprolactone)-*b*-poly-(ethylene oxide) (TAPP-PCL-mPEO) amphiphilic copolymer with tetrakis-(4-aminophenyl)-terminated porphyrin as the core for bioimaging and tumor treatment. The micelles were characterized by dynamic light scattering (DLS) and transmission electron microscopy (TEM). The cellular uptake and in vivo biodistribution of the PTX-loaded micelles were monitored by fluorescent imaging thanks to the inherent fluorescent characteristic of porphyrin moiety. It is found that the PTX-loaded micelles can be readily internalized by cancer cells and have a slightly higher cytotoxicity than the clinic PTX injection Taxol. The in vivo real-time fluorescent imaging revealed that the micelles could accumulate at tumor site via the blood circulation in tumor-bearing mice. In vivo antitumor efficacy examinations indicated that the PTX-loaded micelles had significantly superior efficacy in impeding tumor growth than Taxol and low toxicity to the living mice.

Experimental Section

Materials and Methods

Methoxyl poly(ethylene oxide) (mPEO, $\overline{M}_w = 5\,000$ Da), ε-Caprolactone (ε-CL, Sigma-Aldrich) were purchased from Sigma-Aldrich. Paclitaxel (PTX) was bought from Chongqing Taihao Pharmaceutical Co., LTD. Taxol was purchased from Sichuan Taiji Pharmaceutical Co., LTD. 5, 10, 15, 20-tetrakis-(4-aminophenyl)-21H, 23H-porphine (TAPP) was synthesized following published procedures.[27] The ^{1}H NMR spectra were recorded on a Bruker DPX-300 at 300 MHz. The molecular weight and distribution was measured by size exclusion chromatography (SEC) (Waters 515 pump) equipped with double detectors, including a UV detector (Waters 2487) and a refractive index detector (Wyatt Technology Optilab rEX). The columns were STRAGEL HR3, HR4 and HR5 (300 · 7.8 mm) from waters. THF was used as the mobile phase at a flow rate of 1.0 mL/min. TEM analyses were performed on JEOL JEM-1010 after staining with phosphotungstic acid solution (2%, w/v). Mean diameter and size distribution of the micelles were determined by dynamic light scattering (DLS) method using a Brookheaven BI9000AT system (Brookheaven Instruments Corporation, USA). The fluorescence spectra were taken with RF-5301PC spectrofluorometer (Shimadzu, Japan), and UV-vis absorption spectra were collected using UV3100 spectrophotometer (Shimadzu, Japan). Confocal image was recorded on a Zeiss LSM-710 microscope (Germany). HPLC analysis was performed on a Shimadzu LC-15A (Shimazu, Japan) HPLC system equipped with a Shimadzu UV detector and a C-18 Wondasil-HPLC analysis column. The mobile phase was consisting of acetonitrile:-water (58:42, v/v), and delivered at a flow of 1.0 mL/min at 25 °C. Detection was done at 228 nm. The retention time of PTX was at 5.4 min.

Polymerization of ε-Caprolactone using Porphyrin as Initiator

TAPP (16.85 mg, 0.025 mmol), stannous octoate (1.00 mg, 0.0025 mmol) and ε-caprolactone (0.7 g, 6.14 mmol) were added into a 10 mL flask under Ar. The mixture was allowed to stir at 110 °C for 72 h. After the reaction was complete, the resulting mixture was dissolved in methylene chloride and precipitated into cold methanol. The precipitates were filtered out, washed several times with diethyl ether and dried under vacuum to afford TAPP-PCL (0.645 g, 90%).

Synthesis of Star-Shaped TAPP-PCL-mPEO Copolymer

Carboxyl-terminated methoxyl poly(ethylene oxide) (mPEO-COOH) was synthesized following published procedures.[28] Briefly, mPEO-COOH (125 mg, 0.025 mmol) and TAPP-PCL (140 mg, 0.0052 mmol) were placed into a flask and then the flask was evacuated for 4 h at 90 °C. After the mixture was cooled to room temperature, the solution of 4-(dimethylamino)pyridium 4-toluenesulfonate (DTPS) (6 mg, 0.02 mmol) in 15 mL of dry methylene chloride was added to the reaction mixture under Ar. 1,3-dicyclohexylcarbodiimide (DCC) (12 mg, 0.06 mmol) in 2 mL of dry methylene chloride was also added to the reaction mixture. The solution was stirred at room temperature for 4 d. The resulting mixture was filtered and precipitated into cold diethyl ether. The precipitates were filtered out, washed several times with diethyl ether and dried under vacuum. The solid were dissolved in acetone, and then dropped into distilled water. The organic solvent was removed at room temperature under vacuum. The resultant solution was dialyzed against 1 L of deionized water for 10 h in a dialysis bag (MWCO, 15 000) to remove unreacted mPEO-COOH and other impurities. The obtained suspension was lyophilized to give a solid (224 mg, 92%).

Preparation of Drug-Loaded Micelles

Blank or PTX-loaded micelles were prepared by a modified nanoprecipitation method. 10 mg of TAPP-PCL-mPEO copolymer, with or without 0.75 mg of PTX were dissolved in ethanol (1 mL), and then dropped into 2 mL of hot water (50 °C) under moderate stirring. The ethanol was removed under reduced pressure at room temperature. The suspension was filtered by a 0.22 μm cellulose acetate filter to remove the free PTX.

Drug Loading Content and Encapsulation Efficiency

The lyophilized micelles were accurately weighted before thoroughly dissolved in methanol. The PTX concentration in the resulted methanol solution was determined by HPLC and using a

preestablished calibration curve. The drug loading content and encapsulation efficiency was calculated by the following formulas respectively:

$$\text{Drug loading content \%} = \frac{\text{Weight of the drug in the micelles}}{\text{Weight of the micelles}} \times 100\%$$

$$\text{Encapsulation efficiency \%} = \frac{\text{Weight of drug in the micelles}}{\text{Weight of the feeding drug}} \times 100\%$$

In Vitro Release of PTX-Loaded Micelles

A suspension of the PTX-loaded micelles bearing 150 μg of PTX in water was dialyzed against 10 mL of 1 M sodium salicylate solution at 37 °C in a 15 kDa MWCO membrane. After a predetermined period, 1 mL aliquots were withdrawn and then the same volume of medium was replenshed. The PTX concentration in sampled release medium was determined by HPLC and using a preestablished calibration curve. The measurements were performed in triplicate and the results were the average of the three times.

Cellular Uptake of the PTX-Loaded Micelles

The human colon carcinoma LoVo cells were grown at 37 °C in a humidified atmosphere of 5% CO_2 in Dulbecco's modified Eagle's medium (DMEM). The culture medium was supplemented with 10% fetal calf serum, 100 μg/mL streptomycin, 100 U/mL penicillin and $4 \cdot 10^{-3}$ M L-glutamine. The cells were seeded into a 6-well plate at a density of 2.5×10^5 cells per well and incubated for 12 h. Thereafter, the cells were coincubated with PTX-loaded micelles at

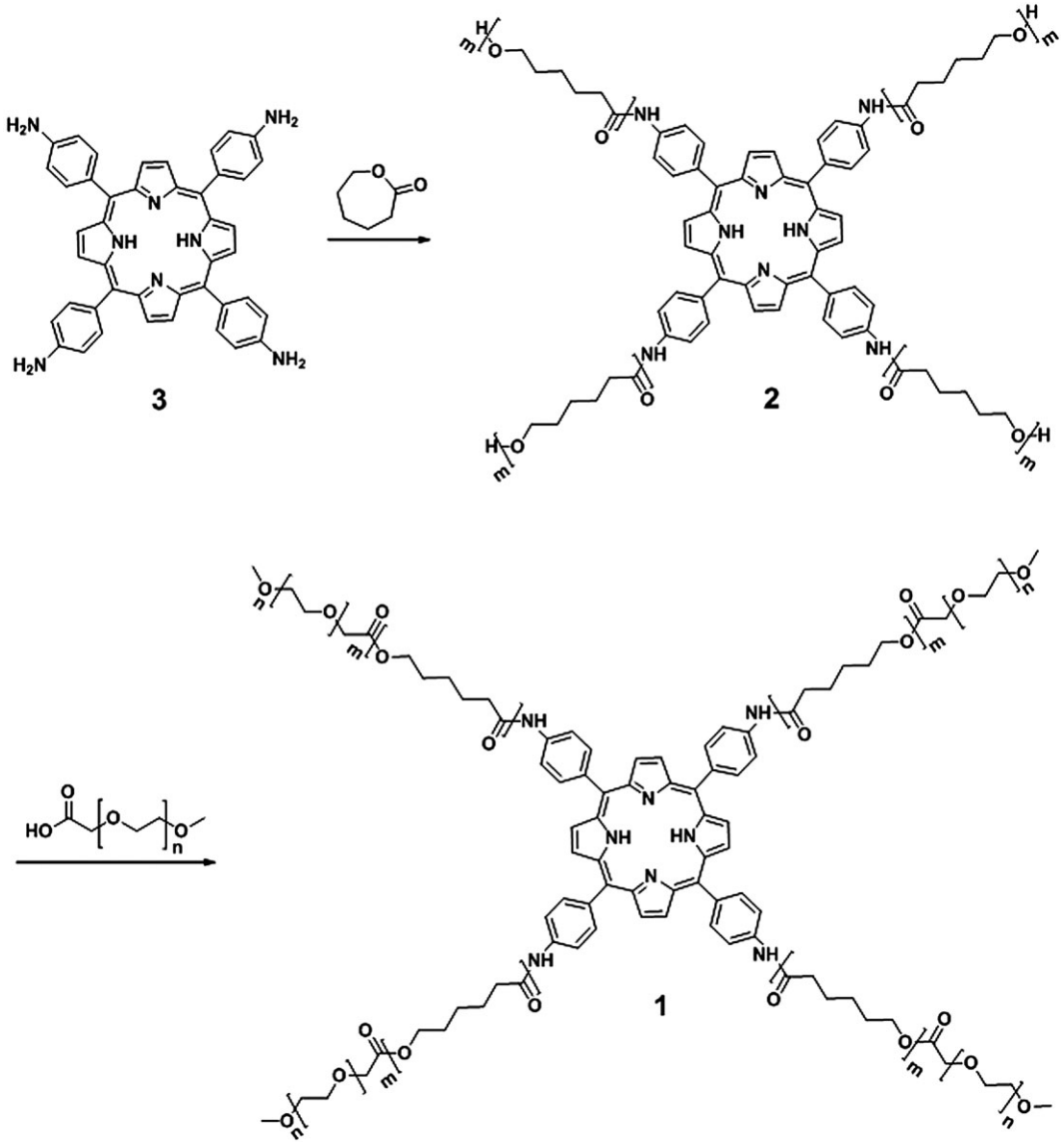

Scheme 1. Synthesis of star-shaped block copolymer.

a final concentration of 40 μg/mL for 4 h at 37 °C. After the incubation, the cells were washed three times with PBS at 4 °C and 37 °C respectively. Then the cells were observed with laser scanning confocal microscopy (LSCM) at an excitation wavelength of 488 nm.

In Vitro Cytotoxity

The cytotoxicity of samples was tested by MTT [3-(4, 5-dimethylthiazol-2-yl)-2, 5-diphenyltetrazolium bromide] assay. LoVo cells were seeded into a 96-well plate at a density of 5 000 cells per well and incubated with 100 μL culture medium containing a series of doses of the samples at 37 °C for 48 h. After the incubation, the culture medium in each well was removed and the cells were washed three times with PBS. 20 μL of MTT solution (5 mg/mL) was added to each well and cultured for another 4 h. The supernatant was discarded and then 100 μL of DMSO was added to each well. The values of the plate were observed on a microplate reader at 570 nm (Safire, Tecan). The results were expressed as the viable percentage of cells after various treatments relative to the control cells without any treatment. Cell viability was calculated by following formula:

$$\text{Cell viability}\,\% = \frac{\text{Absorbance test cells}}{\text{Absorbance controlled cells}} \times 100\%$$

In Vivo Tumor Inhibition of Drug-Loaded Micelles

All animal experiments were performed in accordance with the guidelines for animal experiments and are approved by the Animal Care Committee at Drum Tower Hospital. In order to establish the experimental model of the tumor, H22 tumor cells ($5-6\times10^6$ cells per mouse) were inoculated subcutaneously into the armpit of male ICR mice (6 – 8 weeks, 23 – 30 g, provided by central Animal Laboratory of Nanjing Medical University). When the tumor reached a mean volume of ~50 mm^3, the animals were equally randomized into four groups (six per group): (1) negative control group (saline group); (2) positive control group (Taxol, 5 mg/kg); (3) blank micelles; (4) PTX-loaded micelles (PTX, 5 mg/kg, equiv). 0.3 mL of the control groups or drugs was administrated injection through the tail vein at day 0 and day 7. After administration, the tumor diameters were measured every other day with a vernier caliper in two dimensions and calculated as volume $V = d^2 \times D/2$ (where d is the tumor measurement at the shortest point, and D is the tumor dimension at the longest point). In addition, the body weight of each mouse was determined every other day for safety evaluation of the control and PTX formulations.

The tumor growth inhibition (TGI) was calculated by the following equation:

$$\text{TGI} = \frac{\widetilde{V}\text{ of saline control group} - \widetilde{V}\text{of tested group}}{\widetilde{V}\text{ of saline control group}}$$

In vivo Real-Time Imaging

H22 tumor cells ($5-6\times10^6$ cells/mouse) were inoculated subcutaneously to animals in the armpit region. Tumor growth was monitored until it reached the acceptable sizes. The PTX-loaded micelles were injected into the mice bearing the tumor through a tail vein. The mice were anesthetized with isoflurane at various time points post-injection. The animals were imaged using the Maestro in vivo optical imaging system (CRI, Inc., Woburn, MA). Thereafter, the mice bearing tumor was scarified and tumor, heart, liver, spleen, lung, intestine, stomach were harvested for isolated organ imaging.

Histology Study

On the 16th d after treatment, the animals were sacrificed. The tissues including tumor, heart, liver, spleen, lung and kidney from the test groups treated with PTX-loaded micelles, blank micelles, Taxol and saline were dissected and fixed in 10% neutral buffered formalin. Lastly, the tissues were processed routinely to paraffin, sectioned at 4 μm, stained with hematoxylin and eosin (H&E) and examined by optical microscopy.

Statistical Analysis

Statistical analysis were performed by Student's t-test for the difference of tumor inhibition between the groups treated with PTX-loaded micelles and Taxol at equivalent dose of PTX, and

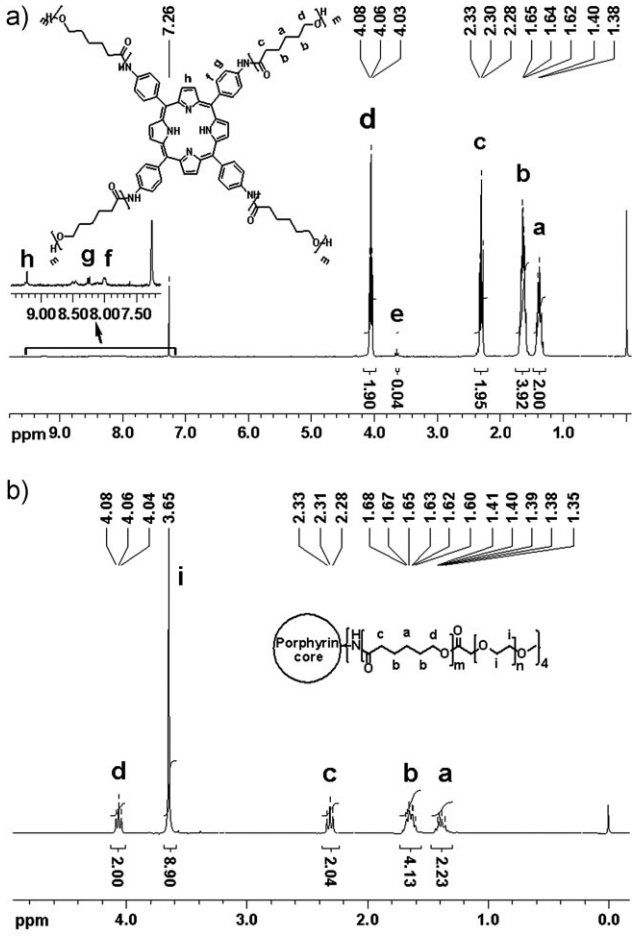

Figure 1. ^{1}H NMR spectrum of (a) TAPP-PCL (**2**), (b) TAPP-PCL-mPEO (**1**).

p values less than 0.05 were statistically significant. All results were expressed as mean ± standard deviation (SD).

Results and Discussion

Synthesis of Star Copolymer and Their PTX-Loaded Micelles

The synthetic route of the TAPP-PCL-mPEO copolymer (**1**) is summarized in Scheme 1. First, hydroxyl-terminated TAPP-PCL (**2**) was synthesized by ring-opening polymerization of ε-caprolactone using TAPP (**3**) as an initiator with the

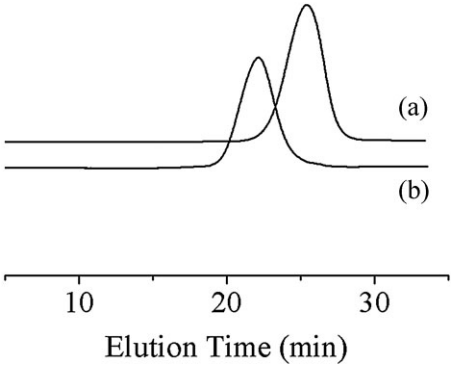

Figure 2. SEC diagram of the synthesized polymers: (a) TAPP-PCL (**2**), (b) TAPP-PCL-mPEO (**1**).

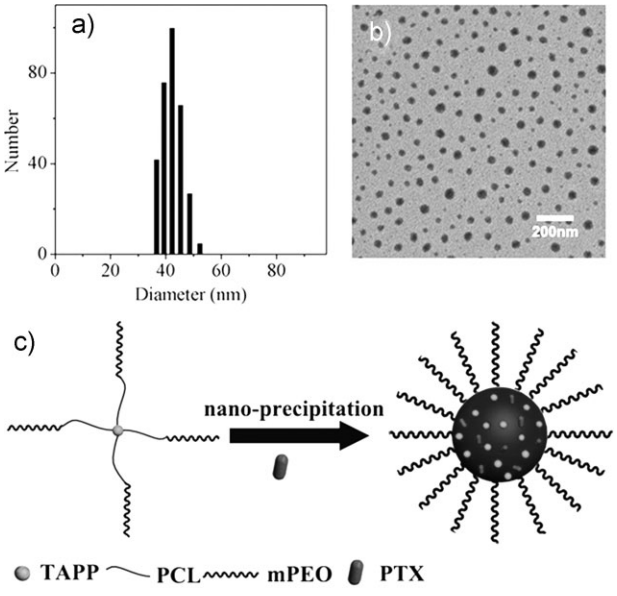

Figure 3. (a) Hydrodynamic diameter distribution of the PTX-loaded micelles determined by DLS. (b) TEM image of the PTX-loaded micelles. (c) Schematic diagram of the preparation of PTX-loaded micelles.

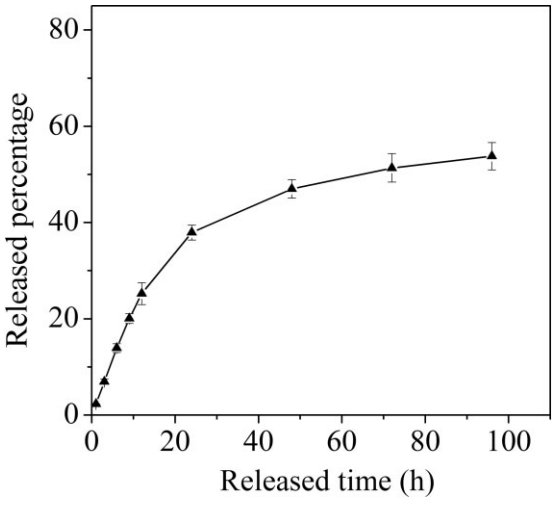

Figure 4. In vitro release profile of PTX-loaded micelles in 1 M sodium salicylate medium at 37 °C. Each point represents mean ±standard.

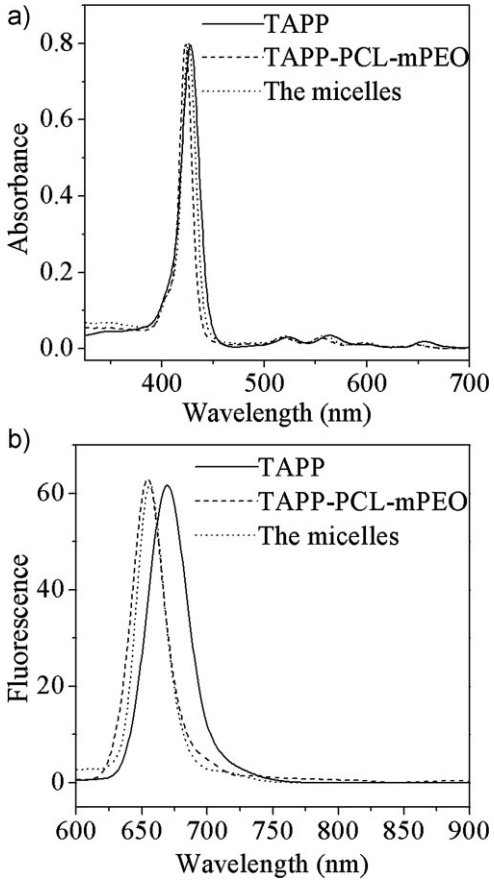

Figure 5. UV-vis absorption (a) and fluorescence emission (b) spectra of TAPP, the TAPP-PCL-mPEO copolymer in CH_2Cl_2 and the micelles in water.

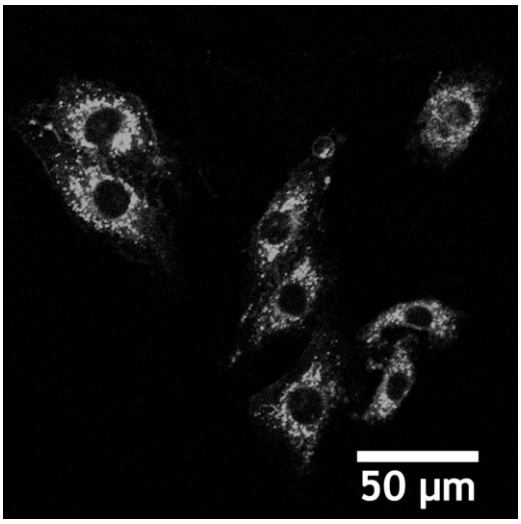

Figure 6. LSCM image of LoVo cells incubated with PTX-loaded micelles for 4 h.

catalyst of stannous octoate.[29] The copolymer was purified by precipitating several times from methylene dichloride into cold methanol. The ^{1}H NMR spectrum of the synthesized TAPP-PCL is shown in Figure 1a. As marked in Figure 1a, the characteristic signals from both PCL (a, 1.39 ppm; b, 1.63 ppm; c, 2.30 ppm; d, 4.05 ppm) and TAPP (f, 7.94 ppm; g, 8.14 ppm; h, 8.85 ppm) moieties can be observed, suggesting the successful synthesis of hydroxyl-terminated TAPP-PCL (**2**). The TAPP-PCL was further combined with mPEO-COOH in presence of 1,3-dicyclohexylcarbodiimide (DCC) and 4-(dimethylamino)pyridium 4-toluenesulfonate (DTPS) to form the star-shaped copolymer TAPP-PCL-mPEO with amphiphilic characteristic. The chemical structure of TAPP-PCL-mPEO was confirmed by ^{1}H NMR spectroscopy (Figure 1b). The molecular weight and polydispersity (PDI) of the TAPP-PCL-mPEO were determined to be 47.8 kDa and 1.386, respectively, by size exclusion chromatography (SEC) (Figure 2), in contrast

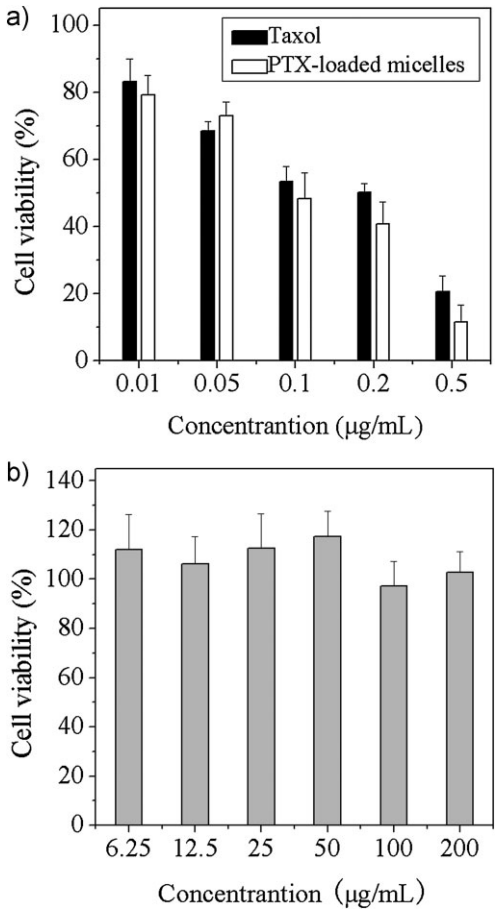

Figure 7. (a) In vitro cytotoxicity of PTX-loaded micelles and Taxol against LoVo cells. (b) In vitro cytotoxicity of blank micelles against LoVo cells.

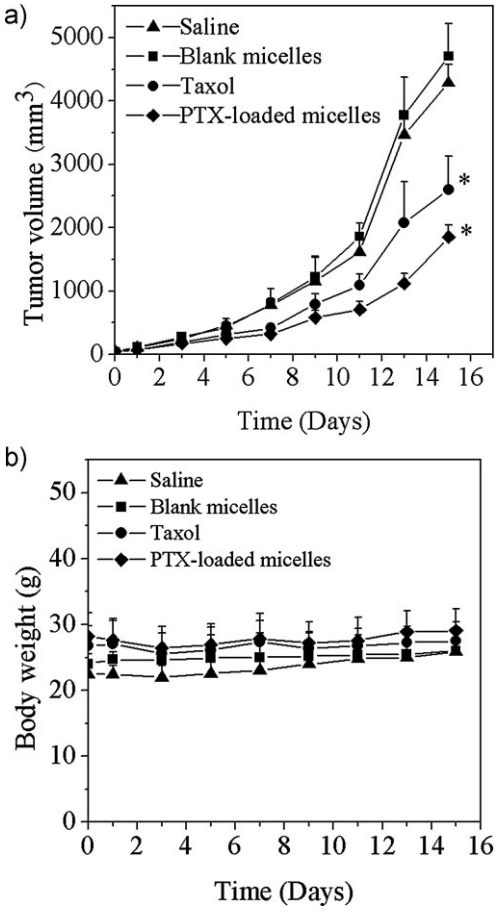

Figure 8. (a) In vivo antitumor effect of saline, blank micelles, Taxol, PTX-loaded micelles in tumor-bearing ICR mice. * $P < 0.05$ since the 5th d. (b) Evolution of body weight of each group during the experiments.

with the molecular weight of 23.4 kDa and PDI of 1.335 for TAPP-PCL.

To evaluate the performance of the TAPP-PCL-mPEO copolymer in fabricating micelles and drug delivery, PTX was selected as a model drug and the PTX-loaded micelles were prepared by a modified nano-precipitation method (see experimental section for detailed procedures). The PTX encapsulation efficiency and loading content was determined to be 89% and 5% respectively. The mean hydrodynamic diameter of the PTX-loaded micelles was determined to be 46 nm by DLS (Figure 3a). The morphological structure of the PTX-loaded micelles was examined by TEM, as shown in Figure 3b. It can be seen that the micelles have a near-spherical shape with a diameter of about 38 ± 15 nm. The diameter determined by TEM is smaller than that by DLS due to the shrinkage in dry state. During the formation of the micelles, the PCL segments and PTX molecules should self-assemble into the hydrophobic core of the micelles, while the PEO segments constitute the hydrophilic shell (Figure 3c, a color image is shown in the Supporting Information).

In vitro Performance of PTX-Loaded Micelles

The in vitro release of PTX from the micelles was examined by using dialysis diffusion method. In order to increase the aqueous solubility of PTX, 1 M sodium salicylate solution was used for the release medium.[30,31] Figure 4 shows the in vitro PTX release profile at 37 °C within 96 h monitoring duration. A sustained release profile is observed without initial burst release. About 53.8% of the loaded PTX is released from the micelles within 96 h.

The inherent fluorescent characteristic of the porphyrin moiety can be used to study the cellular uptake and biodistribution of the PTX-loaded micelles by fluorescent imaging in no need of further labeling. Figure 5 shows the absorption and fluorescence spectra of the TAPP-PCL-mPEO copolymer and TAPP in CH_2Cl_2 and the micelles in water at room temperature. It can be observed that the absorption bands of the copolymer appear at 423, 519, 556, 593, and 650 nm respectively, slightly blue-shifted comparing to that of TAPP. The emission band of the copolymer appears at 655 nm and also displays a blue shift of 14 nm with respect to that of TAPP. After micellization, the spectroscopic property of the micelles is not changed. The UV-Vis absorption and fluorescence of the micelles in water are comparable to those of the copolymer in CH_2Cl_2.

Laser scanning confocal microscopy (LSCM) was used to trace the cellular uptake of the PTX-loaded micelles by taking advantage of the inherited optical characteristic of the micelles, avoiding the artifact arising from the dye release from labeled micelles. Figure 6 (a color image is shown in the Supporting Information) shows the section image of the human colon carcinoma LoVo cells

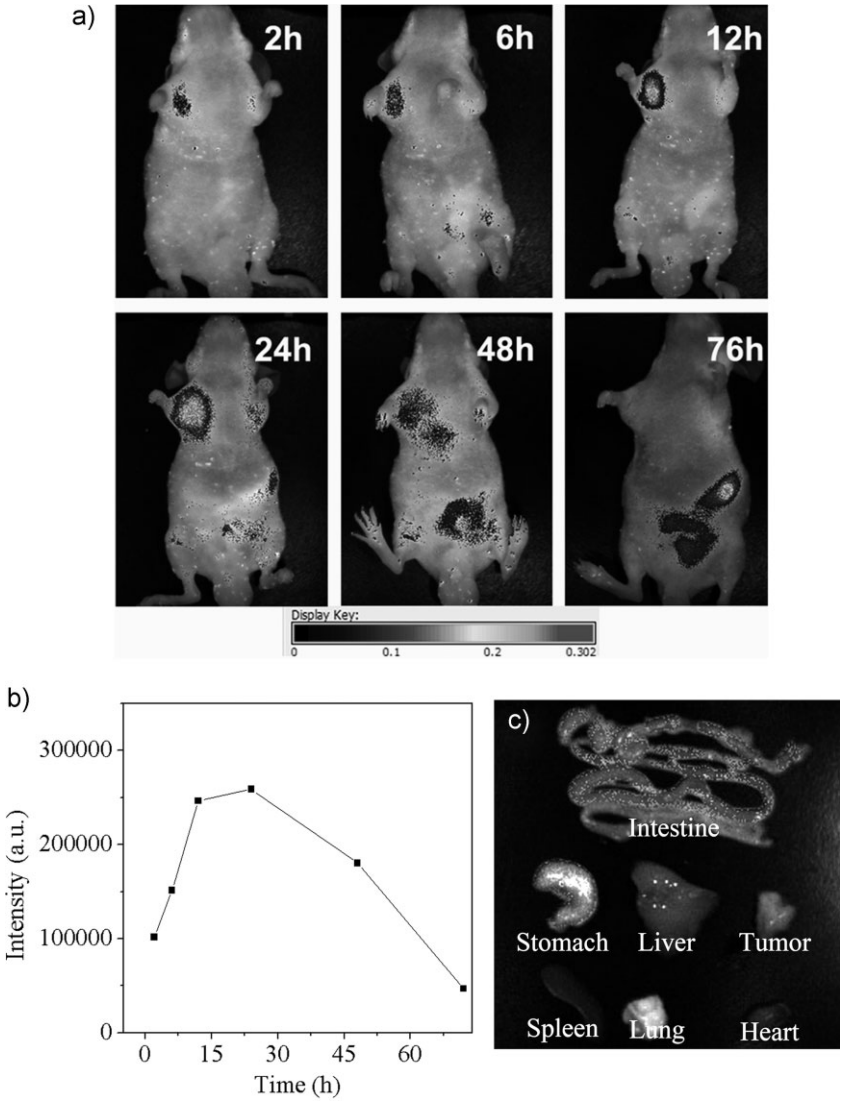

Figure 9. (a) In vivo fluorescence imaging of tumor-bearing mice after intravenous injection of the PTX-loaded micelles. (b) The fluorescence intensity of the region-of-tumor was recorded as total photon counts per tumor corresponding to the fluorescence images in the mice bearing tumor. (c) The fluorescence image of various organs 76 h after intravenous injection.

coincubated with the micelles at 37 °C for 4 h. It is found that the inherent red fluorescence arising from porphyrin moiety of micelles is strong enough and can readily be observed. From the distribution of fluorescence signal in the cells, we found that the micelles are mainly localized in the cytoplasm and all cells maintained their normal morphology. This result suggests that the micelles can be readily internalized by the cells. Also, the tiny spots fluorescence pattern in Figure 6 is indicative of endosomal uptake by the cells through endocytosis.[32]

To examine whether the released PTX is still pharmacologically active, the in vitro cytotoxicity tests of the PTX-loaded micelles against LoVo cells were conducted with clinical Taxol as a positive control (Figure 7). The cell viability was measured by MTT assay after 48 h of incubation with different concentration levels. It can be observed that the PTX-loaded micelles exhibit a slight higher cytotoxicity than Taxol after 48 h exposure in most concentrations. In addition, the cytotoxicity of the blank micelles was also checked and no significant cytotoxicity was found at all used concentrations.

In vivo Antitumor Performance and Toxicity of PTX-Loaded Micelles

The in vivo antitumor performance of the PTX-loaded micelles was further investigated by using murine heparic H22 tumor-bearing mice as the model animals and compared with that of Taxol. The administration is based on the injection through the tail vein at day 0 and day 7, with the dose of 5 mg/kg PTX eq. each injection. Blank micelles and saline were used as negative control. After the treatments, the tumor volumes and weight of the animals were examined and the antitumor effect was evaluated.

Figure 8a shows the variation of the tumor volume with time after the treatments with saline, blank micelles, Taxol and PTX-loaded micelles, respectively. The tumor growth rate of the mice treated with saline is very close to that of the mice treated with the blank micelles. In contrast, significant antitumor effect of the Taxol and PTX-loaded micelles was observed. On the 5th d after administration, the tumors of the group treated with the PTX-loaded micelles are obviously smaller than those of the group treated with Taxol ($P < 0.05$), and this difference in tumor size further enhances with time extension. On the 15th d, the tumor growth inhibition (TGI) calculated for the groups treated with PTX-loaded micelles and Taxol is 56.8% and 39.4%, respectively. In addition, as shown in Figure 8b, the body weights of all the tested groups were examined and exhibited similar evolution profiles during the monitoring period. No serious body weight loss was observed, indicating the well-tolerated dose level of drug and the negligible toxicity of the blank micelles imposed to the experimental mice.

In vivo Real-Time Imaging Studies

To take advantage of the inherent optical characteristic of the micelles, the time-dependent biodistribution in tumor-bearing mice for PTX-loaded micelles was investigated via fluorescence imaging (Figure 9a, a color image is shown in the Supporting Information). The suspensions of the micelles in saline were injected into the murine heparic H22 tumor-bearing mice through tail vein. From Figure 9a, the fluorescence signals can be clearly observed in the tumor region of the mice at 2 h post-injection. The total photon counts in tumor region at different time points were calculated and depicted in Figure 9b. The photon counts in tumor region gradually increase from 2 h post-injection and exhibit a maximum at 24 h post-injection, indicating the accumulation of the micelles in tumor *via* the enhanced permeability and retention (EPR) effect. With further time extension, the fluorescence intensity in the tumor region falls slow down and becomes very weak at 48 h post-injection. Finally, the fluorescence signal in the tumor region cannot be detected at 76 h post-injection, indicating the micelles can be cleared up slowly from the tumor. On the other hand, the fluorescence signals in the intestine and stomach regions can be observed clearly from 48 and 76 h post-injection respectively. To further evaluate the tissue distribution of the micelles, the different organs including heart, liver, spleen, lung, stomach, intestine as well as

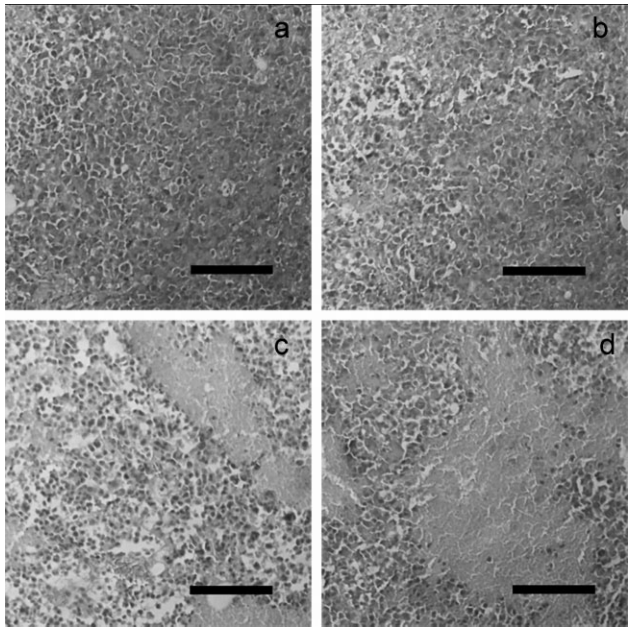

Figure 10. H&E stained tumor slices from mice on the 16th d after treatments with saline (a), blank micelles (b), Taxol (c), the PTX-loaded micelles (d). The scale bar represents 100 μm.

tumor were excised at 76 h post-injection and imaged. It is found that the fluorescence signals can only be observed in the stomach and intestine (Figure 9c, a color image is shown in the Supporting Information), which consists well with the in vivo imaging at 76 h post-injection. Based on the biodistribution evolution of the micelles, it can be speculated that the micelles may be excreted via the hepatobiliary transport and end up in feces.[33,34] Thus, the accumulation of the PTX-loaded micelles in tumor tissue should be responsible for their higher antitumor performance than Taxol.

Histology Studies

To verify the necrosis level in the tumor from the groups treated with saline, blank micelles, Taxol and PTX-loaded micelles, the mice after 15 d of treatments were sacrificed, and the tumors were resected from the mice. The tumor slices were stained by hematoxylin and eosin (H&E) and analyzed via the optical microscopy (Figure 10, a color image is shown in the Supporting Information). Large-area apoptotic or necrotic region can be observed in the PTX-loaded micelles treated tumor. In contrast, the Taxol treated tumors display a much lower apoptotic level with a large amount of living cells existing. The tumor treated with saline and blank micelles exhibited similar parallel and the lowest apoptotic region.

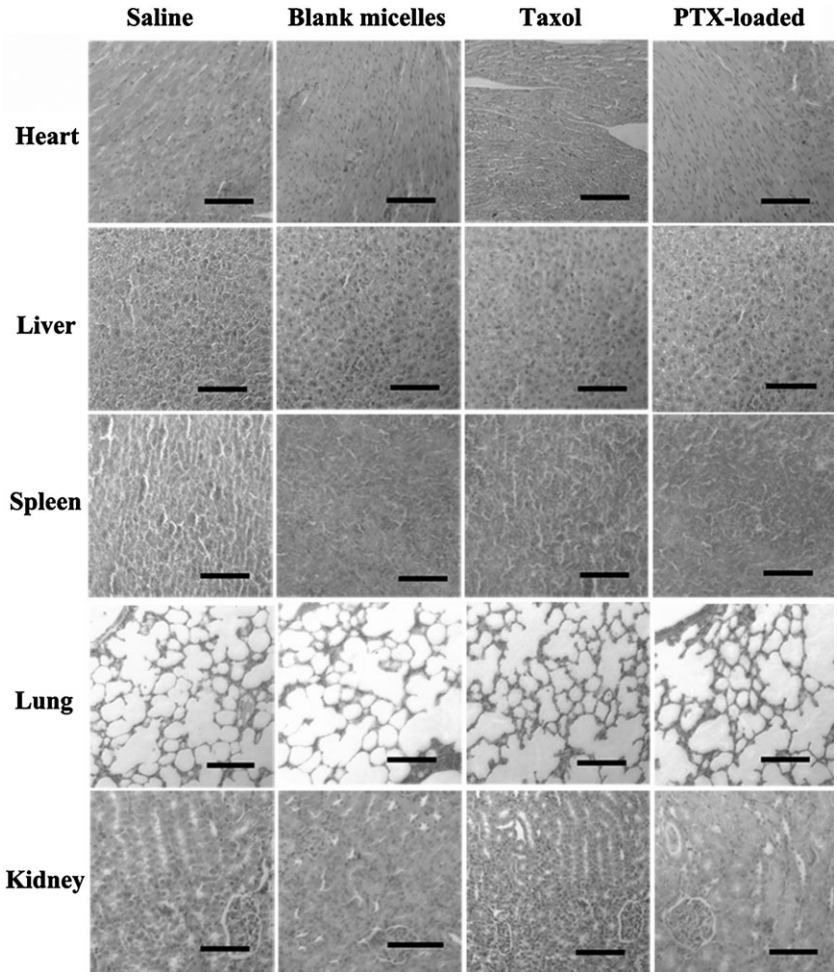

Figure 11. H&E stained heart, liver, spleen, lung, and kidney slices from mice on the 16th d after treatments with PTX-loaded micelles, Taxol, blank micelles, saline. The scale bar represents 100 μm.

In order to investigate the potential toxicity of the PTX-loaded micelles, Taxol and blank micelles to the experimental mice, major organs including heart, liver, spleen, lung and kidney were resected, formalin-fixed and examined under optical microscopy at the completion of the 15 d tumor suppression study (Figure 11, a color image is shown in the Supporting Information). All the injected samples did not cause any significant lesion to the tested organs, suggesting that the micelles injection have negligible effect on the mice.

Conclusion

Star-shaped poly(ε-caprolactone)-*b*-poly(ethylene oxide) (TAPP-PCL-mPEO) amphiphilic copolymer with a porphyrin core was synthesized, and the drug-loaded micelles were prepared by the self-assembly of this star amphiphilic copolymer and in situ encapsulation of PTX. In vitro cytotoxicity tests revealed that the PTX released from the micelles remains its pharmacological activity and showed a slightly higher cytotoxicity than Taxol. In virtue of the inherent fluorescent characteristic of the porphyrin moiety, the cellular uptake and biodistribution of the PTX-loaded micelles can be easily monitored by fluorescent imaging. The in vivo real-time fluorescent imaging revealed that the drug-loaded micelles could accumulate at tumor site via the blood circulation in tumor-bearing mice. In vivo antitumor efficacy examination exhibited significantly superior antitumor effect compared to the Taxol and low toxicity to the living mice.

Acknowledgements: This study was supported by the Natural Science Foundation of China (No. 51033002, 50802040 and 20874042).

Received: May 21, 2011; Published online: August 25, 2011; DOI: 10.1002/mabi.201100197

Keywords: bioimaging; drug delivery; micelles; porphyrin star-shaped copolymer

[1] Z. L. Tyrrell, Y. Q. Shen, M. Radosz, *Prog. Polym. Sci.* **2010**, *35*, 1128.
[2] T. Lammers, V. Subr, K. Ulbrich, W. E. Hennink, G. Storm, F. Kiessling, *Nano Today* **2010**, *5*, 197.
[3] N. Wiradharma, Y. Zhang, S. Venkataraman, J. L. Hedrick, Y. Y. Yang, *Nano Today* **2009**, *4*, 302.
[4] A. S. Mikhail, C. Allen, *J. Control. Release* **2009**, *138*, 214.
[5] L. Qiu, R. Wang, C. Zheng, Y. Jin, L. Q. Jin, *Nanomedicine* **2010**, *5*, 193.
[6] G. Gaucher, M. H. Dufresne, V. P. Sant, N. Kang, D. Maysinger, J. C. Leroux, *J. Control. Release* **2005**, *109*, 169.
[7] J. Roovers, L. L. Zhou, P. M. Toporowski, M. Vanderzwan, H. Iatrou, N. Hadjichristidis, *Macromolecules* **1993**, *26*, 4324.
[8] J. Cheng, J. Ding, Y. Wang, J. Wang, *Polymer* **2008**, *49*, 4784.
[9] Z. Yang, W. Zhang, J. Liu, W. Shi, *Colloid. Surface. B* **2007**, *55*, 229.
[10] Z. Yang, J. Xie, W. Zhou, W. Shi, *J. Biomed. Mater. Res. A* **2009**, *89A*, 988.
[11] P. Dong, X. Wang, Y. Gu, Y. Wang, C. Gong, F. Luo, G. Guo, X. Zhao, Y. Wei, Z. Qian, *Colloid. Surface. A* **2010**, *358*, 128.
[12] S. Qiu, H. Huang, X. Dai, W. Zhou, C. Dong, *J. Polym. Sci. ; Part A: Polym. Chem.* **2009**, *47*, 2009.
[13] M. Mooguee, Y. Omidi, S. Davaran, *J. Pharm. Sci.* **2010**, *99*, 3389.
[14] J. Monkare, R. A. Hakala, M. A. Vlasova, A. Huotari, M. Kilpelainen, A. Kiviniemi, V. Meretoja, K. H. Herzig, H. Korhonen, J. V. Seppala, K. Jarvinen, *J. Control. Release* **2010**, *146*, 349.
[15] D. Li, Y. Ping, F. Xu, H. Yu, H. Pan, H. Huang, Q. Wang, G. Tang, J. Li, *Biomacromolecules* **2010**, *11*, 2221.
[16] T. Mori, A. Ishikawa, Y. Nemoto, N. Kambe, M. Sakamoto, Y. Nakayama, *Bioconjugate Chem.* **2009**, *20*, 1262.
[17] K. I. Fukukawa, R. Rossin, A. Hagooly, E. D. Pressly, J. N. Hunt, B. W. Messmore, K. L. Wooley, M. J. Welch, C. J. Hawker, *Biomacromolecules* **2008**, *9*, 1329.
[18] H. Gao, M. Elsabahy, E. V. Giger, D. K. Li, R. E. Prud'homme, J. C. Leroux, *Biomacromolecules* **2010**, *11*, 889.
[19] C. Peng, M. Shieh, M. Tsai, C. Chang, P. Lai, *Biomaterials* **2008**, *29*, 3599.
[20] T. Ren, A. Wang, W. Yuan, L. Li, Y. Feng, *J. Polym. Sci. ; Part A: Polym. Chem.* **2011**, *49*, 2303.
[21] A. A. Ensign, I. Jo, I. Yildirim, T. D. Krauss, K. L. Bren, *P. Natl. Acad. Sci. USA* **2008**, *105*, 10779.
[22] N. Aratani, D. Kim, A. Osuka, *Accounts Chem. Res.* **2009**, *42*, 1922.
[23] A. Endo, M. Ogasawara, A. Takahashi, D. Yokoyama, Y. Kato, C. Adachi, *Adv. Mater.* **2009**, *21*, 4802.
[24] M. Ethirajan, Y. Chen, P. Joshi, R. K. Pandey, *Chem. Soc. Rev.* **2011**, *40*, 340.
[25] K. Berg, P. K. Selbo, A. Weyergang, A. Dietze, L. Prasmickaite, A. Bonsted, B. O. Engesaeter, E. Angell-Petersen, T. Warloe, N. Frandsen, A. Hogset, *J. Microsc. -Oxford* **2005**, *218*, 133.
[26] J. F. Lovell, C. S. Jin, E. Huynh, H. Jin, C. Kim, J. L. Rubinstein, W. C. W. Chan, W. Cao, L. V. Wang, G. Zheng, *Nat. Mater.* **2011**, *10*, 324.
[27] A. Bettelheim, B. A. White, S. A. Raybuck, R. W. Murray, *Inorg. Chem.* **1987**, *26*, 1009.
[28] A. Fishman, A. Acton, E. Lee-Ruff, *Synth. Commun.* **2004**, *34*, 2309.
[29] C. Hua, S. Peng, C. Dong, *Macromolecules* **2008**, *41*, 6686.
[30] H. Xin, L. Chen, J. Gu, X. Ren, Z. Wei, J. Luo, Y. Chen, X. Jiang, X. Sha, X. Fang, *Int. J. Pharm.* **2010**, *402*, 238.
[31] Y. W. Cho, J. Lee, S. C. Lee, K. M. Huh, K. Park, *J. Control. Release* **2004**, *97*, 249.
[32] A. Verma, O. Uzun, Y. H. Hu, Y. Hu, H. S. Han, N. Watson, S. L. Chen, D. J. Irvine, F. Stellacci, *Nat. Mater.* **2008**, *7*, 588.
[33] R. Kumar, I. Roy, T. Y. Ohulchanskky, L. A. Vathy, E. J. Bergey, M. Sajjad, P. N. Prasad, *Acs Nano* **2010**, *4*, 699.
[34] J. S. Souis, C. Lee, S. Cheng, C. Chen, C. Yang, J. A. Ho, C. Mou, L. Lo, *Biomaterials* **2010**, *31*, 5564.